www.revistageintec.net
ISSN: 2237-0722
revista GEINTEC Gestão, Inovação e Tecnologias

Image Denoising Using Low Rank Matrix Approximation in Singular Value Decomposition

V.V. Satyanarayana Tallapragada[1]; G.V. Pradeep Kumar[2]; D. Venkat Reddy[3]; K.L. Narasihimhaprasad[4]

[1]Associate Professor, Department of ECE, Sree Vidyanikethan Engineering College, Tirupati, India.
[1]satya.tvv@gmail.com

[2]Assistant Professor, Department of ECE, Chaitanya Bharathi Institute of Technology, Hyderabad, India.
[2]Pradeepgv16@gmail.com

[3]Professor, Department of ECE, Mahatma Gandhi Institute of Technology, Gandipet, Hyderabad, India.
[3]dasari.reddy@gmail.com

[4]Assistant Professor, Department of ECE, Mallareddy College of Engineering and Technology, Hyderabad, India.
[4]prasad9866@gmail.com

Abstract

The factorization of a matrix into lower rank matrices give solutions to a wide range of computer vision and image processing tasks. The inherent patches or the atomic patches can completely describe the whole image. The lower rank matrices are obtained using different tools including Singular Value Decomposition (SVD), which is typically found in minimization problems of nuclear norms. The singular values obtained will generally be a thresholder to realize the nuclear norm minimization. However, soft-thresholding is performed uniformly on all the singular values that lead to a similar importance to all the patches whether it is principal/useful or not. Our observation is that the decision on a patch (to be principal/useful or not) can be taken only when the application of this minimization is taken into consideration. Thus, in this paper, we propose a new method for image denoising by choosing variable weights to different singular values with a deep noise effect. Experimental results illustrate that the proposed weighted scheme performs better than the state-of-the-art methods.

Key-words: Image Denoising, Low Rank Matrix, Nuclear Norm, Singular Value, Soft-thresholding.

1. Introduction

Low rank matrix (LRM) factorization is a crucial method in data analysis and representation. The raw data have a hidden configuration, and by revealing this configuration, an efficient representation of the data is feasible. This is the vital part of LRM factorization. When the original

image represented in a matrix is factorized into low rank matrices, egresses will be opened for a better matrix completion, data denoising, clustering and dimension reduction. This factorization has many attractive features which make it ideal to many tasks of image processing, though it is not completely developed and applied. This factorization uncovers the inherent structures while answering the sparseness problem associated with many raw data [1]. The solution for this factorization can be done using numerous optimization algorithms like gradient methods. It has strong statistical interpretation.

The LRM factorizations are mainly of three types. They are basic, non-negative, orthogonal non-negative. The constraints imposed in non-negative and orthogonal non-negative are very much useful in many specific circumstances. The basic factorization is formulated as,

$$\min_{U,V} \left\| X - UV^T \right\| + L(U,V) \qquad (1)$$

Here, $X \in R^{m \times n}$ is the matrix to be estimated, $U \in R^{m \times k}$, $V \in R^{n \times k}$ are 2D matrices and L is the regularizing factor [2]. The non-negative factorization tries to represent the data matrix X using lower dimensional matrices, say U and V, which contains only non-negative elements. Now, the problem can be restated as follows.

$$\min_{U,V} O = \left\| X - UV^T \right\|_F^2 + \alpha \|U\|_F^2 + \beta \|V\|_F^2 \qquad (2)$$

where In $\|.\|_F$ is Frobenius norm, α and β are the weights of Frobenius norms of matrices U and V. In addition to the advantage of revealing, the non-negative factorization requires less computational facility. There are few fixed schemes to obtain larger learning rates than the regular gradient based schemes. The orthogonal non-negative factorization requires the U and V to be orthogonal in addition to non-negative. The problem is formulated as follows.

$$\min_{U,V} O = \left\| X - UV^T \right\|_F^2 \qquad (3)$$

The orthogonality condition waives of the regularization terms. The orthogonal non-negative factorization is proved to be equivalent to K-means clustering [3][4]. The LRM factorization has been in wide range of applications and in this paper its application to retrieval of degraded image is explored. Effective algorithms were proposed on denoising, including total variation [5], non-local means method [6] and block matching and 3D filtering [7]. The total-variation method tends to smooth out sharp edges and complexity of BM3D is very high. Consequent works deliberated sparse based methods, leading to better results [8]-[11]. The description and forming the dictionary common

to all input images as well as sub-dictionaries to specific input image plays crucial role in sparse techniques. For instance, [12] assessed the sparse domain coefficients by extracting the self-similarity in the degraded image.

More recently, many sparse representation models focus on learning dictionaries from external database first. Then, the dictionary objects are clustered into few clusters. Then, from these clusters, sub-dictionaries are being formed based on the features of the observed image, hence realizing the real adaptive dictionary. Advantage of adaptively learning sub-dictionary to each input image or to each patch of input image is that the self-structural information is exploited well. As the patches collected from the noisy input image will contain the obvious noise, the sub-dictionary learned may not be the most accurate one. Correspondingly, the performance of the sparse-based models is limited.

In this paper, a method for denoising is proposed using variable weights to different singular values. This method is designed with high amount of noise into consideration. Description of a matrix using low rank matrices provides solution to problems in many applications of image processing. SVD is one concept which can provide the low rank matrices accurately, which is originally used in nuclear norm minimization problems. It is observed that the decision on a patch can be taken only when the application of this minimization is considered.

2. Back Ground

LRM approximation aims to retrieve the low-rank matrix from its degraded version. It has large number of applications in machine learning and compute vision. For example, the low rank matrix generated from facial pictures of humans, makes it possible to restore the ruined faces in the image [13-15]. Low rank matrix data are common in real time. For instance, nonlocal similar patches in natural images [16], Netflix customer data [17] and video captured [18, 19] are all found to have low rank features. In all these kinds of applications the LRM approximation scheme can enable high quality image restoration tasks. In recent years with the rapid development of convex based optimization schemes, many important algorithms are reported in the literature [20, 21]. The LRM approximation schemes can be broadly categorized into two groups: LRM factorization schemes [22, 23] and nuclear-norm minimum (NNM) schemes [24-26].

Given an input matrix X, LRM factorization intends to calculate another matrix Y which is very nearby to X under stipulated conditions. Another constraint on this representation is that the

matrix should be factorized into multiplication of two low rank matrices. A large number of LRM factorization schemes were proposed in the literature. These range from techniques based on singular value decomposition to L_1-norm robust LRM factorization algorithms [27-28]. In nuclear-norm minimization, first, nuclear-norm of matrix Y, $\|Y\|_*$ is defined as follows

$$\|Y\|_* = \sum_j \left|\sigma_j(Y)\right|_1, \tag{4}$$

Here σ denotes singular values and 'j' recognizes specific patch. The aim of nuclear-norm minimization schemes is to get the lowest nuclear-norm while approximating X by Y. One distinct advantage of nuclear-norm minimization is that it is the close-fitting convex moderation to the non-convex LRM factorization. Candes and Recht showed that many LRMs can be seamlessly recuperated by unraveling nuclear-norm minimization problem [25]. Cai, Cand`es, and Z. Shen ascertained that Nuclear-norm Minimization based LRM approximation problem can be straight forwardly resolved using soft-thresholding on singular values [28]. It means the solution of $\hat{Y} = \arg\min_X \|X - Y\|_F^2 + \lambda\|Y\|_*$ is given by $\hat{Y} = US_\lambda(\Sigma)V^T$.

Here λ is a positive constant, $X = U\Sigma V^T$ and $S_\lambda(\Sigma)$ is the soft thresholding function on the diagonal matrix Σ. The singular value soft thresholding was applied to solve numerous nuclear-norm minimization based problems, like representations with low rank for subspace clustering [14], low rank textures [29], robust PCA analysis [18, 21] and matrix completion [25, 30].

Though the nuclear-norm minimization is found to be used in many applications, it suffers from many limitations. Each singular value is treated in a similar way, which results in shrinking all of them by same factor when soft thresholdig is applied [20]. This neglects the prior knowledge which is available on singular values. The soft thresholding scheme associated with nuclear-norm minimization fails to take the benefit of such prior information. Zhang, Hu, Ye, Li, and He presented a truncated NNM model [31]. But the truncated NNM is not very much suitable as it gives a binary decision. To develop the flexibility, in this paper, a weighted NNM is proposed. The weighted nuclear-norm of the matrix Y is defined as

$$\|Y\|_{w,*} = \sum_j \left|w_j\sigma_j(Y)\right|_1 \tag{5}$$

Here **w** =[w_1, w_2, … , w_n] and $w_i \geq 0$ is a weight associated with $\sigma_j(Y)$. The weighted NNM is difficult to solve that the problem of NNM. Also, only a little work was reported in the literature as on now. In this paper, the problem of weighted NNM will be analyzed in depth with F-norm data

Received: 04.03.2021 – Accepted: 10.04.2021

fidelity. The outcomes with different weights are studied and used to the problem of image denoising. Though image denoising is a classical and fundamental issue which has been comprehensively studied, it is quite a lively field. In contemporary years, image nonlocal self-similarity (NSS) exploitation has open the doors to the solutions to denoising [32-34]. From the concept of NSS, for a known local patch in a natural image, one can find numerous alike patches. A local patch refers to the patch of interest which will be processed and alike patch refers to the patch with less distance in similarity. NSS has been a driving force to many successful and popular schemes like NCSR [35], LSSC [36] and BM3D [37]. The traditional NNM was used in video denosing [38]. Dong, Shi, and Li proposed a scheme which combines $L_{2,1}$-norm and NNM for restoration of degraded images.

3. Proposed Method

a. Weighted NNM

The nuclear norm has certain conditions that are satisfied. These conditions are presented in this section with an insight into the application of it in image processing tasks. Consider the matrices P, Q, R and S. For all P, Q that belong to R, that satisfy $P^TQ = 0$,

$$\|P+Q\|_{w,*} \geq \|P\|_{w,*} \tag{6}$$

$$\|P+Q\|_F \geq \|P\|_F \tag{7}$$

For all M, $M = \begin{bmatrix} P & Q \\ R & S \end{bmatrix}$ with $p \in R^{m \times m}$ and $S \in R^{n \times n}$, and if $w_1 \geq \cdots \geq w_{m+n} \geq 0$, then

$\|M\|_{W,*} \geq \|P\|_{W_1,*} + \|S\|_{W_2,*}$ Here $W = [w_1, \cdots w_{m+n}]$, $W_1 = [w_1, \cdots w_m]$ *and* $W_2 = [w_{m+1}, \cdots w_{m+n}]$

For all $P \in R^{nXn}$ and a diagonal matrix $W \in R^{n \times n}$ with descending ordered elements at diagonal and assume that $P = R\Phi S^T$ be the SVD of P, then

$$\sum_i \sigma_i(P)\sigma_i(W) = \max_{U^TU = I, V^TV = I} tr\left[WU^TPV\right] \tag{8}$$

Here $\sigma_i(P)$, $\sigma_i(W)$ are the singular values of P and W and I is the identity matrix. If U = P and V = Q, then $tr\left[WU^TPV\right]$ touches its peak value.

Now, for all $Q \in R^{m\ X\ n}$, which is given by SVD as $Q = U\Sigma V^T$. With a nonnegative weight w, its solution for the problem of weighted NNM, $\hat{Y}$ is given as $\hat{Y} = U\hat{H}V^T$ where $\hat{H}$ can be calculated as

$\hat{H} = \arg\min_H \|\Sigma - H\|_F^2 + \|H\|_{w,*}$. Based on the above, the global solution for weighted NNM is feasible and is given below. When the weights satisfy $w_1 \geq \cdots \geq w_{m+n} \geq 0$, the solution is given by $\hat{Y} = US_w(\Sigma)V^T$ where $X = U\Sigma V^T$ is the SVD representation of X, and $S_w(\Sigma)$ is the soft thresholding operation with weight w. $S_w(\Sigma)_{jj} = \max(\Sigma_{jj} - w_i, 0)$.

If the weights $w_{i=1,\ldots,n}$ are in descending order, then a global minimum is not readily available. Let $B = P\Lambda Q^T$ as the SVD representation of B. Using the non-negative orthogonal LRM factorization, the following optimization will be solved.

$$(\hat{P}, \hat{\Lambda}, \hat{Q}) = \arg\min_{P,\Lambda,Q} \|P\Lambda Q^T - \Sigma\|_F^2 + \|P\Lambda Q^T\|_{w,*} \quad (9)$$

Here P and Q are orthogonal. The final estimation becomes $\hat{Y} = U\hat{P}^T S_w(\Sigma)\hat{Q}V^T$, When the weights are in ascending order, then the estimate becomes $\hat{X} = US_w(\Sigma)V^T$.

b. Image Denoising using Weighted NNM

The objective of image denoising is to recover the original image from its degraded version y = x + n, where n is presumed as an additive white Gaussian noise with zero-mean and variance σ_n^2. The popular work of Buades, B. Coll, and J.-M. Morel initiated an extensive study of NSS approaches for image denoising [32]. NSS signifies that there exists several repeated local patterns across a natural image. The phenomenon for denoising is that those similar patches of a patch which was lost in the process of noise, can be used to reconstruct the lost patch. The NSS methods like NCSR [35], LSSC [36], BM3D [37] and weighted coding with non-local similarity [40] have produced the state-of-the-art results.

Methods like block matching [37] can be used to identify the similar non-local patches for a given local patch. Stacking the nonlocal similar patches into a matrix results in X_i. Then $X_i = Y_i + N_i$. Here Y_i and N_i are the respective patch matrices of initial image and noise. Essentially, Y_i should be a low rank matrix. Hence the LRM approximation schemes should be employed to assess Y_i from X_i. By the accumulation of all unknown or degraded patches, the complete image can be reconstructed. Certainly, the nuclear norm minimization schemes are implemented for video denoising [38]. In this paper, the proposed weighted NNM scheme to estimate Y_i from X_i to yield image denoising. The algorithm is give below.

Algorithm

Step 1: Define the energy functional $\hat{Y}_i = \arg\min_{Y_i} \frac{1}{\sigma_n^2}\|X_i - Y_i\|_F^2 + \|Y_i\|_{w,*}$

Step 2: Define the weight to $\sigma_j(Y_i)$, the j^{th} singular value of Y_i, inversely proportional to the variance, i.e., $w_j = c\sqrt{n_{SP}}/\left(\sigma_j(Y_i)+\varepsilon\right)$

Step 3: Estimate the initial singular value by $\hat{\sigma}_j(Y_i) = \sqrt{\max\left(\sigma_j^2(X_i) - n_{SP}\sigma_n^2, 0\right)}$

Step 4: Accumulate the all the patches to get reconstructed image.

The variance of noise σ_n^2 will be used as normalization factor and the energy function is

$$\hat{Y}_i = \arg\min_{Y_i} \frac{1}{\sigma_n^2}\|X_i - Y_i\|_F^2 + \|Y_i\|_{w,*} \quad (10)$$

Evidently, the crucial concern is to find the weight vector w. For natural images, the larger singular values are more useful than smaller singular values. The large singular values are characterize the energy associated with major components of Y_i. In denoising, when the singular values are large, they should be shrunk less. Hence the weight to $\sigma_j(Y_i)$, the j^{th} singular value of Y_i, should be inversely proportional to the variance. The weight is defined to be,

$$w_j = c\sqrt{n_{SP}}/\left(\sigma_j(Y_i)+\varepsilon\right) \quad (11)$$

Here c is a positive constant, $\varepsilon = 10^{-16}$ and n_{SP} is the number of nonlocal similar patches in X_i. The above weight can be used in the proposed weighted NNM model to perform image denoising. One problem still left is that the singular values $\sigma_j(Y_i)$ are not existing.

Here the assumption is that the noise is distributed evenly over the subspace spanned by the pair U and V, and the initial singular value is estimated as

$$\hat{\sigma}_j(Y_i) = \sqrt{\max\left(\sigma_j^2(X_i) - n_{SP}\sigma_n^2, 0\right)} \quad (12)$$

When $\hat{\sigma}_j(Y_i)$ is sorted in ascending order, the corresponding weights will be guaranteed to be in descending order. By accumulating the patches obtained by following the above procedure, the image can be restored.

4. Experimental Results

This section is devoted to the experimental results obtained. A large number of test images are considered. In the experimentation, different levels of noise was considered and in this section the

results with standard deviation is varied from 10 to 100. The beauty of the proposed scheme is that even when the standard deviation of noise is as high as 100, the performance is better than many state-of-the-art schemes. The peak signal to noise ratio (PSNR) of degraded image for a standard deviation of 10, 25, 50, and 100 is found to be around 28.1 deciBels (dB), 20.14dB, 14.12dB and 8.1dB respectively. Number of iterations and patch size are set based on noise level. For higher noise level, we need to choose bigger patches and run more times the iteration. By experience, we set patch size to 6 X 6, 7 X 7, 8 X 8 and 9 X 9 for $\sigma_n \leq 20$, $20 < \sigma_n \leq 40$, $40 < \sigma_n \leq 60$ and $60 < \sigma_n$, respectively. The performance of the weighted NNM when standard deviation is 10, 25, 50 and 100 is given in Tables 1, 2, 3 and 4 correspondingly.

Table 1- PSNR (in dB) obtained in each iteration when standard deviation of noise is 10

Iteration	**House**	**Pepper**	**Monarch**	**Airplane**	**Lena**	**Barbara**	**Boat**	**Goldhill**	**Man**
Noisy	28.1	28.1	28.1	28.14	28.14	28.14	28.14	28.14	28.14
1	33.97	32.65	32.57	33.65	34.11	32.92	32.43	32.33	31.86
2	35.81	33.89	33.81	35.31	36.06	34.26	33.46	33.31	32.64
3	36.54	34.54	34.51	35.96	36.85	34.98	33.93	33.76	32.98
4	36.75	34.77	34.81	36.16	37.06	35.29	34.05	33.86	33.07
5	36.83	34.84	34.95	36.23	37.13	35.42	34.08	33.87	33.09
6	36.86	34.86	35.01	36.26	37.16	35.49	34.08	33.85	33.08
7	36.87	34.87	35.03	36.26	37.17	35.51	34.08	33.83	33.06
8	36.86	34.86	35.04	36.25	37.17	35.52	34.07	33.81	33.05

Table 2- PSNR (in dB) obtained in each iteration when standard deviation of noise is 25

Iteration	**House**	**Pepper**	**Monarch**	**Airplane**	**Lena**	**Barbara**	**Boat**	**Goldhill**	**Man**
Noisy	20.14	20.14	20.14	20.18	20.18	20.18	20.18	20.18	20.18
1	26.15	23.01	25.09	26.04	26.62	25.56	25.51	25.55	25.12
2	29.22	25.71	27.12	28.93	29.58	27.96	27.79	27.86	27.04
3	31.6	27.80	28.66	30.97	31.66	29.84	29.37	29.46	28.28
4	32.42	28.52	29.37	31.55	32.26	30.67	29.85	29.88	28.65
5	32.77	28.83	29.65	31.74	32.45	30.99	29.98	29.97	28.74
6	32.95	28.99	29.76	31.81	32.52	31.14	30.02	29.99	28.75
7	33.07	29.09	29.81	31.83	32.54	31.21	30.04	30	28.75
8	33.14	29.16	29.83	31.84	32.55	31.24	30.04	30	28.74

Table 3- PSNR (in dB) obtained in each iteration when standard deviation of noise is 50

Iteration	House	Pepper	Monarch	Airplane	Lena	Barbara	Boat	Goldhill	Man
Noisy	14.12	14.12	14.12	14.16	14.16	14.16	14.16	14.16	14.16
1	19.38	16.99	18.83	19.45	20.08	19.18	19.24	19.34	19.09
2	22.36	19.61	21.16	22.48	23.20	21.86	21.98	22.19	21.61
3	26.1	22.89	23.62	26.13	26.97	24.88	25.03	25.44	24.27
4	28.41	24.91	25.21	27.88	28.78	26.71	26.51	26.97	25.52
5	29.22	25.62	25.81	28.3	29.21	27.33	26.83	27.23	25.8
6	29.58	25.94	26.05	28.43	29.35	27.55	26.91	27.29	25.87
7	29.79	26.12	26.16	28.49	29.41	27.66	26.94	27.32	25.9
8	29.93	26.24	26.21	28.53	29.45	27.72	26.95	27.34	25.92

Table 4- PSNR (in dB) obtained in each iteration when standard deviation of noise is 100

Iteration	House	Pepper	Monarch	Airplane	Lena	Barbara	Boat	Goldhill	Man
Noisy	8.1	8.1	8.1	8.14	8.14	8.14	8.14	8.14	8.14
1	12.76	12.64	12.53	12.87	12.95	12.76	12.82	12.88	12.76
2	15.24	14.98	14.74	15.45	15.63	15.19	15.31	15.45	15.18
3	18.76	18.06	17.58	19.2	19.7	18.52	18.85	19.18	18.49
4	22.86	21.25	20.47	23.27	24.66	22.02	22.55	23.21	21.82
5	24.97	22.79	21.93	24.68	26.61	23.55	23.78	24.47	23.02
6	25.63	23.27	22.4	24.96	26.97	23.94	23.96	24.64	23.25
7	25.94	23.49	22.61	25.1	27.13	24.12	24.03	24.71	23.35
8	26.1	23.6	22.71	25.17	27.2	24.21	24.06	24.74	23.4

Interestingly the techniques resulted in a very close PSNR for different input images. This is because the low rank matrices which constitute the complete image will be from the same set of low rank matrices. The noise effect is less when the standard deviation is 10, hence the lower rank matrices of most of the images will be similar, and this is somehow analogous to the atomic structure of any particles.

But when the noise effect is high, the set of low rank matrices required to represent all the images will be large. As a consequence, the results obtained with more noise by the means of a standard deviation of 100 will be somehow different with different input images. The same can be observed from the Table 2. Figures 1 and 2 shows input, degraded and denoised images with noise standard deviation of 10. The corresponding images are shown in Figures 3 and 4 for standard deviation of 100. The degradation as expected is too high with the noise standard deviation of 100. As it is evident from the Figures 3 and 4, the reconstructed image can well serve many applications. The performance of the proposed method is plotted in Figure 5. The Table 5 and 6 give the performance comparison of denoising by proposed method with the state-of-the-art techniques. In most of the cases, the proposed method gives better results compared to the remaining methods.

Figure 1- Results of Weighted NNM method with noise standard deviation 10 for input images1 to 5

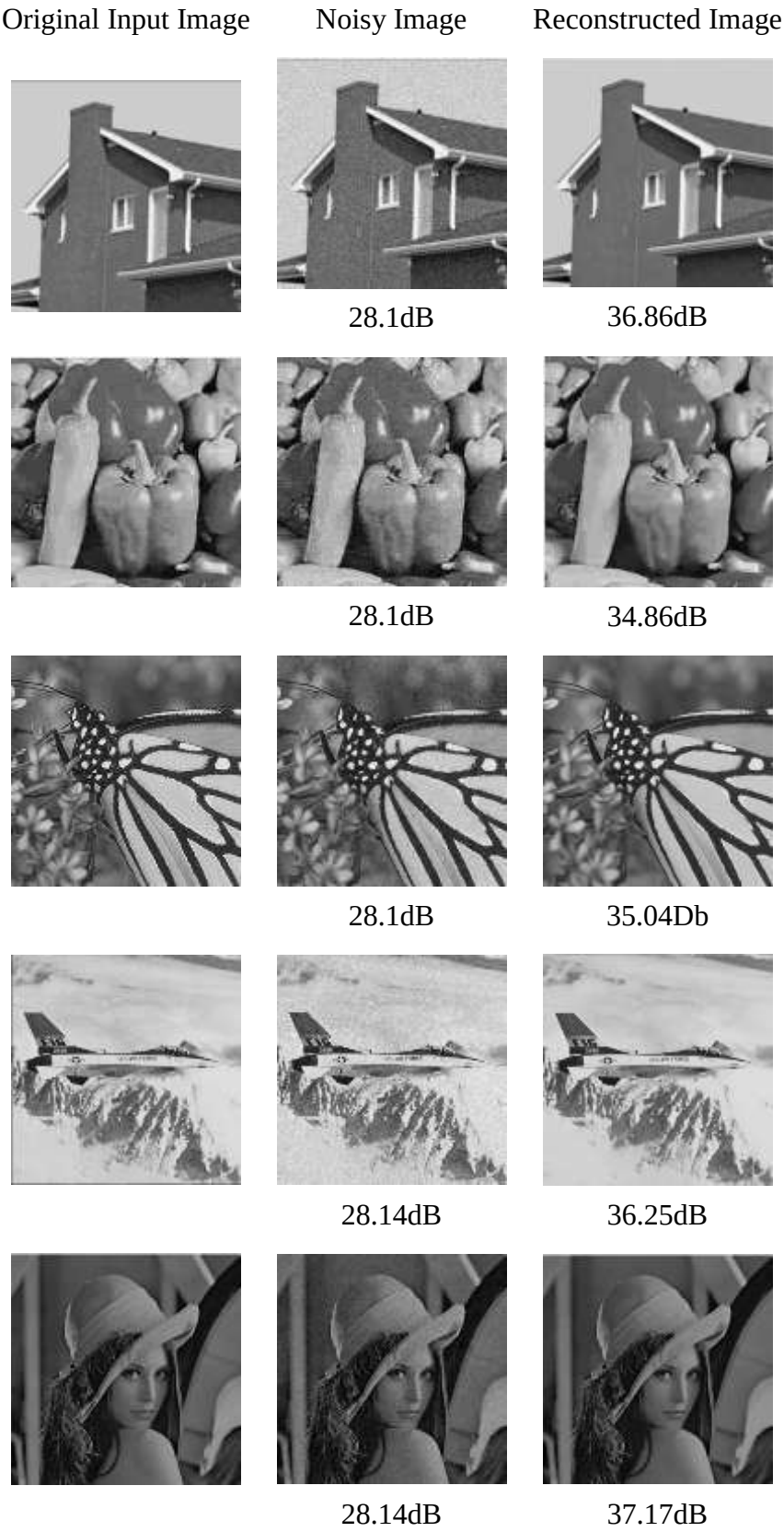

Figure 2- Results of Weighted NNM method with noise standard deviation 10 for input images6 to 10

Received: 04.03.2021 – Accepted: 10.04.2021

Figure 3- Results of Weighted NNM method with noise standard deviation 100 for input images 1 to 5

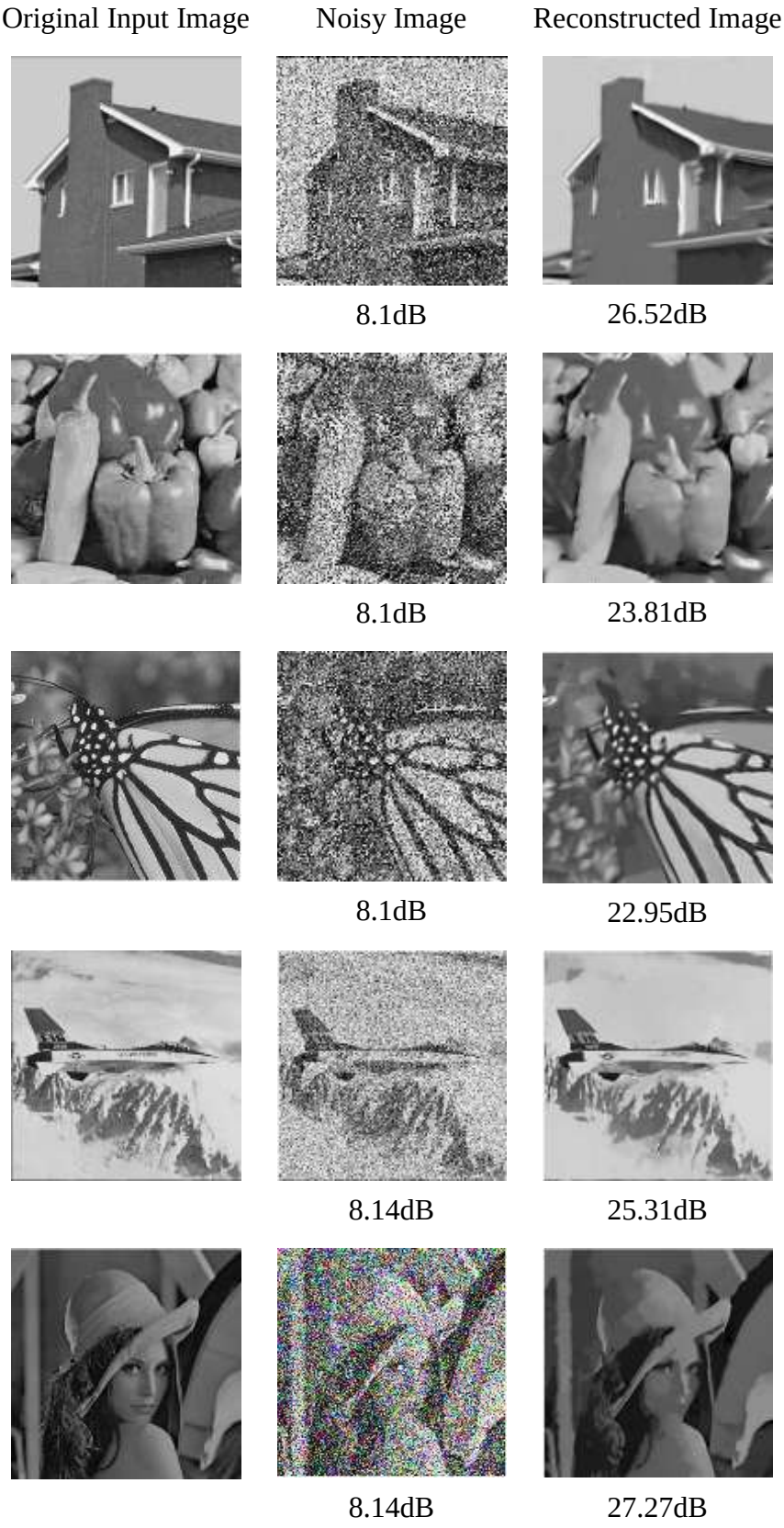

Received: 04.03.2021 – Accepted: 10.04.2021

Figure 4- Results of Weighted NNM method with noise standard deviation 100 for input images 6 to 10

Received: 04.03.2021 – Accepted: 10.04.2021

Figure 5- PSNR (dB) with different values of Noise Standard Deviation

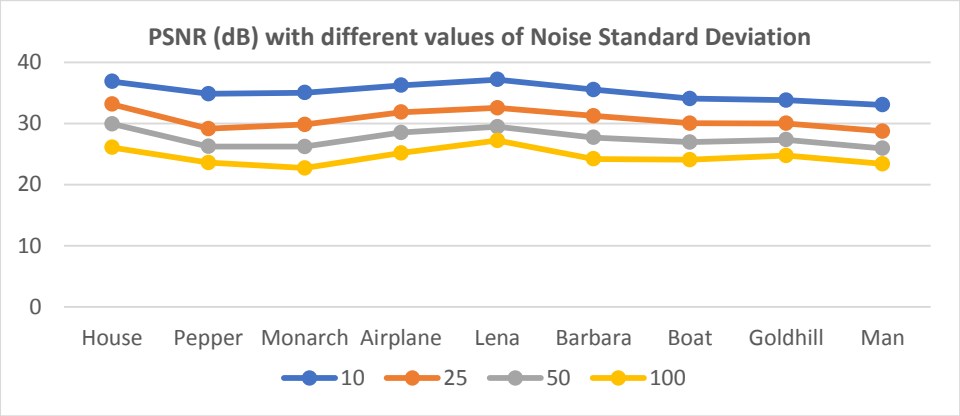

Table 5- Denoising results (PSNR) by different methods for standard deviation of 10

Method	House	Pepper	Monarch	Airplane	Lena	Barbara	Boat	Goldhill	Couple
NNM[24]	35.97	33.77	33.54	32.19	35.19	34.40	33.05	32.89	32.97
BM3D[37]	36.71	34.68	34.12	33.33	35.93	34.98	33.92	33.62	34.04
EPLL[39]	35.75	34.54	34.27	33.39	35.58	33.61	33.66	33.48	33.85
LSSC[36]	**36.95**	34.80	34.44	33.51	35.83	34.98	34.01	33.66	34.01
NCSR[35]	36.80	34.68	34.51	33.40	35.85	35.00	33.91	33.69	34.00
SAIST[34]	36.66	34.82	34.76	33.43	35.90	35.24	33.91	33.65	33.96
Proposed	36.86	**34.86**	**35.04**	**36.25**	**37.17**	**35.52**	**34.07**	**33.81**	**34.13**

Table 6- Denoising results (PSNR) by different methods for standard deviation of 100

Method	House	Pepper	Monarch	Airplane	Lena	Barbara	Boat	Goldhill	Couple
NNM[24]	23.65	21.24	20.22	20.73	24.41	22.14	22.48	23.32	22.07
BM3D[37]	25.87	23.39	22.52	22.11	25.95	23.62	23.97	24.58	23.51
EPLL[39]	25.19	23.08	22.23	22.02	25.30	22.14	23.71	24.43	23.32
LSSC[36]	25.71	23.20	22.24	21.69	25.96	23.54	23.87	24.47	23.27
NCSR[35]	25.56	22.84	22.11	21.83	25.71	23.20	23.68	24.36	23.15
SAIST[34]	**26.53**	23.32	22.61	22.27	25.93	24.07	23.80	24.29	23.21
Proposed	26.52	**23.81**	**22.95**	**25.31**	**27.27**	**24.37**	**24.11**	**24.77**	**23.56**

5. Conclusion

In this paper, the low-rank matrix factorization was extended and improved nuclear norm minimization was proposed. The low rank matrix representation was shown to be an efficient way of representing whole image, and the set of these matrices is very less as compared to the whole image. In addition, the low rank matrices are shown to restore similar patches degraded by noise effect. To highlight the restoring or replicating phenomenon of low rank matrices, image denoising was taken as an application. The LRM based nuclear norm minimization was enhanced by including a weight to

the singular values by that enabling different importance to different singular values. Deep additive white Gaussian noise up to a standard deviation of 100 is considered. The experimental results showed a clear improvement of the performance of the proposed technique over other state-of-the-art methods.

References

Koren, Y. (2008). Factorization meets the neighborhood: a multifaceted collaborative filtering model. *In Proceedings of the 14th ACM SIGKDD international conference on Knowledge discovery and data mining*, 426-434.

Hastie, T., Tibshirani, R., & Friedman, J. (2009). *The elements of statistical learning: data mining, inference, and prediction.* Springer Science & Business Media.

Ding, C., He, X., & Simon, H.D. (2005). On the equivalence of nonnegative matrix factorization and spectral clustering. *In Proceedings of the 2005 SIAM international conference on data mining, Society for Industrial and Applied Mathematics*, 606-610.

Ding, C., Li, T., Peng, W., & Park, H. (2006). Orthogonal nonnegative matrix t-factorizations for clustering. *In Proceedings of the 12th ACM SIGKDD international conference on Knowledge discovery and data mining*, 126-135.

Afonso, M., & Sanches, J.M. (2015). Image reconstruction under multiplicative speckle noise using total variation. *Neurocomputing, 150*, 200-213.

Sun, Z., Chen, S., & Qiao, L. (2014). A general non-local denoising model using multi-kernel-induced measures. *Pattern recognition, 47*(4), 1751-1763.

Dabov, K., Foi, A., Katkovnik, V., & Egiazarian, K. (2009). BM3D image denoising with shape-adaptive principal component analysis. *In SPARS'09-Signal Processing with Adaptive Sparse Structured Representations.*

Liu, J., Huang, T.Z., Lv, X.G., & Wang, S. (2017). High-order total variation-based Poissonian image deconvolution with spatially adapted regularization parameter. *Applied Mathematical Modelling, 45*, 516-529.

Miao, C.Q. (2018). Computing eigenpairs in augmented Krylov subspace produced by Jacobi–Davidson correction equation. *Journal of Computational and Applied Mathematics, 343*, 363-372.

Ma, W.X., & Zhou, Y. (2018). Lump solutions to nonlinear partial differential equations via Hirota bilinear forms. *Journal of Differential Equations, 264*(4), 2633-2659.

Jiang, C., Zhang, F., & Li, T. (2018). Synchronization and antisynchronization of N‐coupled fractional‐order complex chaotic systems with ring connection. *Mathematical Methods in the Applied Sciences, 41*(7), 2625-2638.

Dong, W., Zhang, L., Shi, G., & Li, X. (2012). Nonlocally centralized sparse representation for image restoration. *IEEE transactions on Image Processing, 22*(4), 1620-1630.

De La Torre, F., & Black, M.J. (2003). A framework for robust subspace learning. *International Journal of Computer Vision, 54*(1), 117-142.

Liu, G., Lin, Z., & Yu, Y. (2010). Robust subspace segmentation by low-rank representation. *International Conference on Machine Learning, Israel, 1*(8).

Zheng, Y., Liu, G., Sugimoto, S., Yan, S., & Okutomi, M. (2012). Practical low-rank matrix approximation under robust l_1-norm. *In IEEE Conference on Computer Vision and Pattern Recognition*, 1410-1417.

Wang, S., Zhang, L., & Liang, Y. (2012). Nonlocal spectral prior model for low-level vision. *In Asian Conference on Computer Vision*, 231-244.

Salakhutdinov, R., & Srebro, N. (2010). Collaborative filtering in a non-uniform world: Learning with the weighted trace norm. *Neural Information Processing Systems Conference.*

Wright, J., Ganesh, A., Rao, S., & Ma, Y. (2009). Robust principal component analysis: Exact recovery of corrupted low-rank matrices via convex optimization. *Neural Information Processing Systems Conference.*

Mu, Y., Dong, J., Yuan, X., & Yan, S. (2011). Accelerated low-rank visual recovery by random projection. *International Conference on Computer Vision and Pattern Recognition*, 2609-2616.

Fazel, M., Hindi, H., & Boyd, S. P. (2001). A rank minimization heuristic with application to minimum order system approximation. *In Proceedings of the 2001 American Control Conference. (Cat. No. 01CH37148), 6*, 4734-4739.

Candès, E.J., Li, X., Ma, Y., & Wright, J. (2011). Robust principal component analysis? *Journal of the ACM (JACM), 58*(3), 1-37.

Srebro, N., & Jaakkola, T. (2003). Weighted low-rank approximations. *In Proceedings of the 20th International Conference on Machine Learning (ICML-03)*, 720-727.

Buchanan, A.M., & Fitzgibbon, A.W. (2005). Damped newton algorithms for matrix factorization with missing data. *In IEEE Computer Society Conference on Computer Vision and Pattern Recognition (CVPR'05), 2*, 316-322.

Lin, Z., Liu, R., & Su, Z. (2011). Linearized alternating direction method with adaptive penalty for low-rank representation. *Neural Information Processing Systems Conference*.

Liu, R., Lin, Z., De la Torre, F., & Su, Z. (2012). Fixed-rank representation for unsupervised visual learning. *In IEEE Conference on Computer Vision and Pattern Recognition*, 598-605.

Donoho, D. L., Gavish, M., & Montanari, A. (2013). The phase transition of matrix recovery from Gaussian measurements matches the minimax MSE of matrix denoising. *Proceedings of the National Academy of Sciences, 110*(21), 8405-8410.

Ke, Q., & Kanade, T. (2005). Robust l_1 norm factorization in the presence of outliers and missing data by alternative convex programming. *In IEEE Computer Society Conference on Computer Vision and Pattern Recognition (CVPR'05)*, 1, 739-746.

Cai, J. F., Candès, E. J., & Shen, Z. (2010). A singular value thresholding algorithm for matrix completion. *SIAM Journal on optimization, 20*(4), 1956-1982.

Zhang, Z., Ganesh, A., Liang, X., & Ma, Y. (2012). TILT: Transform invariant low-rank textures. *International journal of computer vision, 99*(1), 1-24.

Candes, E.J., & Plan, Y. (2010). Matrix completion with noise. *Proceedings of the IEEE, 98*(6), 925-936.

Zhang, D., Hu, Y., Ye, J., Li, X., & He, X. (2012). Matrix completion by truncated nuclear norm regularization. *In IEEE Conference on Computer Vision and Pattern Recognition*, 2192-2199.

Buades, A., Coll, B., & Morel, J.M. (2005). A non-local algorithm for image denoising. *In IEEE Computer Society Conference on Computer Vision and Pattern Recognition (CVPR'05), 2*, 60-65.

Elad, M., & Aharon, M. (2006). Image denoising via sparse and redundant representations over learned dictionaries. *IEEE Transactions on Image processing*, *15*(12), 3736-3745.

Dong, W., Shi, G., & Li, X. (2012). Nonlocal image restoration with bilateral variance estimation: a low-rank approach. *IEEE transactions on image processing*, *22*(2), 700-711.

Mairal, J., Bach, F., Ponce, J., Sapiro, G., & Zisserman, A. (2009, September). Non-local sparse models for image restoration. *In IEEE 12th international conference on computer vision*, 2272-2279.

Dabov, K., Foi, A., Katkovnik, V., & Egiazarian, K. (2007). Image denoising by sparse 3-D transform-domain collaborative filtering. *IEEE Transactions on image processing*, *16*(8), 2080-2095.

Ji, H., Liu, C., Shen, Z., & Xu, Y. (2010). Robust video denoising using low rank matrix completion. *In IEEE Computer Society Conference on Computer Vision and Pattern Recognition*, 1791-1798.

Zoran, D., & Weiss, Y. (2011). From learning models of natural image patches to whole image restoration. *In International Conference on Computer Vision*, 479-486.

Tallapragada, V.S., Manga, N.A., Kumar, G.P., & Naresh, M.V. (2020). Mixed image denoising using weighted coding and non-local similarity. *SN Applied Sciences*, *2*(6), 1-11.

https://doi.org/10.1007/s42452-020-2816-y